Comparison of dose calculation methods for brachytherapy of intraocular tumors

Mark J. Rivard[a)]
Department of Radiation Oncology, Tufts University School of Medicine, Boston, Massachusetts 02111

Sou-Tung Chiu-Tsao
Quality MediPhys LLC, Denville, New Jersey 07834

Paul T. Finger
The New York Eye Cancer Center, New York, New York 10065

Ali S. Meigooni
Department of Radiation Oncology, Comprehensive Cancer Center of Nevada, Las Vegas, Nevada 89169

Christopher S. Melhus
Department of Radiation Oncology, Tufts University School of Medicine, Boston, Massachusetts 02111

Firas Mourtada
Department of Radiation Physics, University of Texas, M.D. Anderson Cancer Center, Houston, Texas 77030 and Department of Experimental Diagnostic Imaging, University of Texas, M.D. Anderson Cancer Center, Houston, Texas 77030

Mary E. Napolitano
Physics, Elekta Inc., Norcross, Georgia 30092

D. W. O. Rogers and Rowan M. Thomson
Department of Physics, Carleton University, Ottawa, Ontario K1S 5B6 Canada

Ravinder Nath
Department of Therapeutic Radiology, Yale University School of Medicine, New Haven, Connecticut 06520

(Received 16 July 2010; revised 10 November 2010; accepted for publication 11 November 2010; published 21 December 2010)

Purpose: To investigate dosimetric differences among several clinical treatment planning systems (TPS) and Monte Carlo (MC) codes for brachytherapy of intraocular tumors using ^{125}I or ^{103}Pd plaques, and to evaluate the impact on the prescription dose of the adoption of MC codes and certain versions of a TPS (Plaque Simulator with optional modules).
Methods: Three clinical brachytherapy TPS capable of intraocular brachytherapy treatment planning and two MC codes were compared. The TPS investigated were Pinnacle v8.0dp1, BrachyVision v8.1, and Plaque Simulator v5.3.9, all of which use the AAPM TG-43 formalism in water. The Plaque Simulator software can also handle some correction factors from MC simulations. The MC codes used are MCNP5 v1.40 and BrachyDose/EGSnrc. Using these TPS and MC codes, three types of calculations were performed: homogeneous medium with point sources (for the TPS only, using the 1D TG-43 dose calculation formalism); homogeneous medium with line sources (TPS with 2D TG-43 dose calculation formalism and MC codes); and plaque heterogeneity-corrected line sources (Plaque Simulator with modified 2D TG-43 dose calculation formalism and MC codes). Comparisons were made of doses calculated at points-of-interest on the plaque central-axis and at off-axis points of clinical interest within a standardized model of the right eye.
Results: For the homogeneous water medium case, agreement was within ~2% for the point- and line-source models when comparing between TPS and between TPS and MC codes, respectively. For the heterogeneous medium case, dose differences (as calculated using the MC codes and Plaque Simulator) differ by up to 37% on the central-axis in comparison to the homogeneous water calculations. A prescription dose of 85 Gy at 5 mm depth based on calculations in a homogeneous medium delivers 76 Gy and 67 Gy for specific ^{125}I and ^{103}Pd sources, respectively, when accounting for COMS-plaque heterogeneities. For off-axis points-of-interest, dose differences approached factors of 7 and 12 at some positions for ^{125}I and ^{103}Pd, respectively. There was good agreement (~3%) among MC codes and Plaque Simulator results when appropriate parameters calculated using MC codes were input into Plaque Simulator. Plaque Simulator and MC users are perhaps at risk of overdosing patients up to 20% if heterogeneity corrections are used and the prescribed dose is not modified appropriately.
Conclusions: Agreement within 2% was observed among conventional brachytherapy TPS and MC codes for intraocular brachytherapy dose calculations in a homogeneous water environment. In general, the magnitude of dose errors incurred by ignoring the effect of the plaque backing and

Silastic insert (i.e., by using the TG-43 approach) increased with distance from the plaque's central-axis. Considering the presence of material heterogeneities in a typical eye plaque, the best method in this study for dose calculations is a verified MC simulation. © *2011 American Association of Physicists in Medicine*. [DOI: 10.1118/1.3523614]

Key words: COMS, eye plaque, brachytherapy, dosimetry, Monte Carlo simulations, TG-43, intraocular tumors

I. INTRODUCTION

Recent advances in dose calculation methods have drawn attention to limitations of the current AAPM TG-43 dosimetry formalism under certain circumstances.[1–3] Dosimetry of eye plaques (used for the treatment of intraocular tumors) is one of these circumstances because of the following reasons: significant material inhomogeneities relative to water are involved, the eye is a small structure (~2.5 cm diam.), and the points of interest are at distances as close as 1 mm from the radioactive sources. Furthermore, investigations have demonstrated that dose distributions in the eye are critical in determining location and incidence of side-effects.[4,5]

Prior to 1986, there was no consensus approach for radiotherapy of choroidal melanoma resulting in the use of widely different techniques at various institutions. At that time, the Collaborative Ocular Melanoma Study (COMS), a multi-institutional cooperative clinical trial sponsored by the National Eye Institute of the National Institutes of Health (Bethesda, MD), was started. The COMS trial compared enucleation against a minimum of 100 Gy ^{125}I plaque radiation therapy for medium-sized choroidal melanomas (i.e., between 2.5 mm and 10 mm in height and $<$16 mm basal diameter).[6,7] With no difference in survival found between treatment arms after 12 years of follow up, the COMS clearly established ^{125}I plaque brachytherapy as an effective eye- and vision-sparing treatment for choroidal melanoma.[8] The most recent publications on trial outcomes can be found in COMS Reports Nos. 24 and 28 published in 2004 and 2006, respectively.[8,9] In 1996, the dose prescription of 100 Gy (based on pre-TG-43 dosimetry) was revised to 85 Gy following the introduction of the TG-43 formalism.[10,11] This dose was prescribed to the tumor apex when the tumor apex was $\geq$5 mm, and to 5 mm when the tumor apex was $<$5 mm. In 2003, the American Brachytherapy Society recommended prescribing to the tumor apex for all medium-sized choroidal melanomas, even those $<$5 mm in height.[12]

In the 1990s, Chiu-Tsao *et al.*[13,14] and de la Zerda *et al.*[15] reported thermoluminescent dosimeter (TLD) measurements and Monte Carlo (MC) radiation transport simulations of the dose distributions in an eye phantom for a single ^{125}I and ^{103}Pd source in a COMS-plaque. These groups observed central-axis dose reductions of ~10% and ~16% for ^{125}I and ^{103}Pd, respectively, and off-axis dose reductions up to 30%. They attributed these reductions to the presence of the plaque's Silastic insert (silicone polymer seed carrier) and the gold-alloy (Modulay) backing (where the term backing includes the plaque collimating lip). Being 40% silicon by weight, Silastic has an effective-atomic number Z_{eff}=10.7 (substantially greater than that of water at 7.42 or air at 7.63) and consequently attenuates low-energy photons more than water via the photoelectric effect.

The COMS medium-tumor trial dosimetry was reanalyzed by Krintz *et al.* in 2003 to investigate the impact of source anisotropy, the line-source approximation for the geometry function, radiation collimation by the plaque gold-alloy lip, and 10% dose reduction by the Silastic insert using an earlier version of Astrahan's Plaque Simulator (PS) software (distributed by IBt Bebig, Berlin, Germany).[16,17] The reanalysis determined that corrected dose calculations resulted in a significant and consistent reduction of between 7% and 21% compared to COMS-calculated values for points of interest within the eye; supporting the earlier results of Chiu-Tsao *et al.*[13] Based on the TG-43 algorithm with a semianalytical method to incorporate additional scatter and attenuation factors, PS accounts for the effects of the gold-alloy backing and attenuation from the Silastic. More recent versions of PS software[18] included the correction factors which depend on the path length of primary radiation in Silastic and gold-alloy and the distance between the calculation point and radioactive seed. For fully loaded 12 mm and 20 mm plaques, Astrahan reconfirmed in 2005 that the calculated doses to critical ocular structures ranged from 16% to 50% less than would have been reported using the standard COMS dose calculation protocol.

Older MC radiation transport codes such as those using MORSE had limited geometry packages, physics models, and computing power.[13] However, current MC codes take advantage of more powerful computing systems that allow the simulation of complex brachytherapy environments such as eye plaques.[19,20] The objective of this study is to present a dosimetric comparison of modern MC simulations and conventional brachytherapy treatment planning systems (TPSs) using a 16 mm diameter COMS plaque (Fig. 1). The current study focuses on the impact of modern MC methods on the administered dose for the treatment of intraocular tumors.

II. MATERIALS AND METHODS

Three TG-43-based TPS capable of intraocular radiotherapy planning (Pinnacle v8.0dp1,[21] BrachyVision v8.1,[22] and PS v5.3.9) (Ref. 18) and two MC codes [MCNP5 v1.40 (Ref. 23) and BrachyDose/EGSnrc (Refs. 24 and 25)] were used in this study. With these TPS and MC codes, three types of calculations were performed.

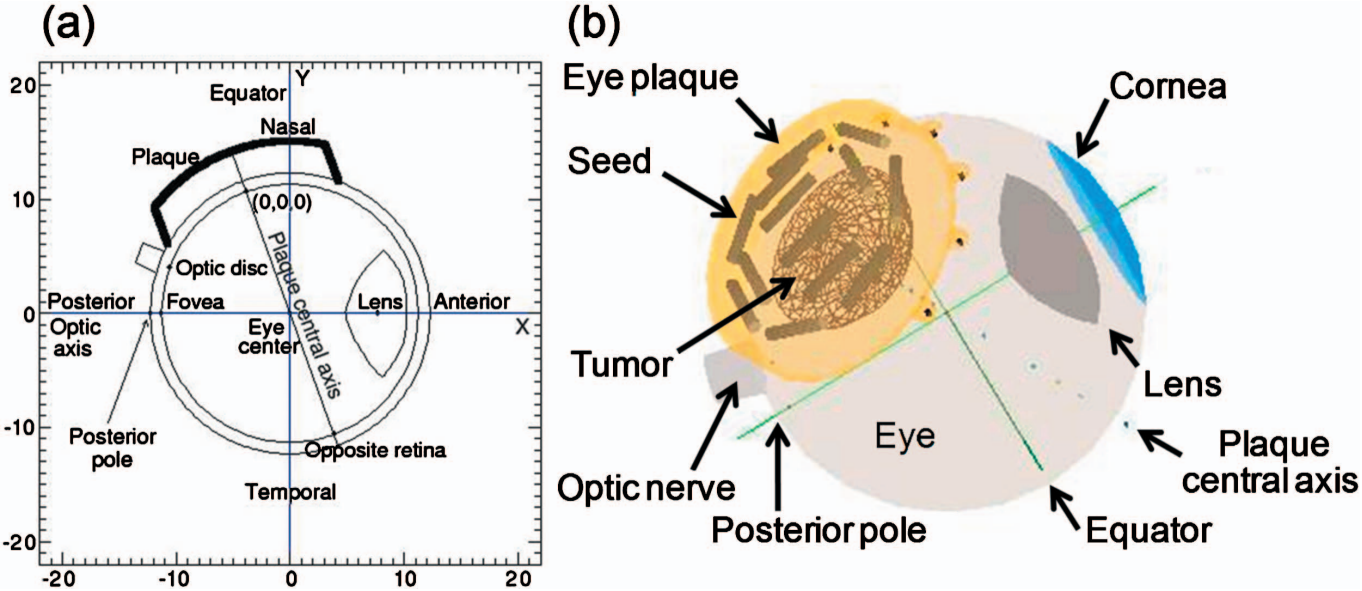

FIG. 1. (a) Diagram of a standard eye model in the horizontal plane for a 16 mm COMS eye plaque viewed from a superior perspective. Illustrated here are the locations (millimeters) of the points-of-interest examined in this study. (b) 3D view of a 16 mm eye plaque applied on the surface of the standard eye viewed from a superior-medial perspective. The posterior edge of the plaque is placed against the optic nerve, corresponding to Fig. 1(a) and position #6 of Fig. 3.

(1) *Point source in homogeneous media.*

(a) Point-Homo: Superposition of dose contributions from single seeds based on the point-source approximation (TG-43 1D formalism), excluding dosimetric anisotropy effects in an unbounded, homogeneous water phantom according to the original COMS protocol.

(2) *Line source in homogeneous media.*

(a) Line-Homo: Superposition of dose contributions from single seeds based on the line-source approximation (TG-43 2D formalism) in an unbounded, homogeneous water phantom.

(b) MC-Homo: Dose distributions from seeds in an unbounded, homogeneous water phantom using MCNP5 and BrachyDose (with no interseed effects) were calculated for comparison to the TG-43-based calculations, i.e., (2a).

(3) *Line source in heterogeneous media.* This approach accounted for radiological perturbations by the gold-alloy backing and the Silastic insert.

(a) PS-Hetero: Superposition of single seed 2D dose contributions based on the line-source approximation in an unbounded water phantom with a semianalytical correction for plaque attenuation and scatter (using input from MC simulations) was performed using for comparison to the full MC simulations, i.e., (3b).

(b) MC-Hetero: Full MC simulations of detailed models of all seeds (including interseed effects) and the plaque (gold-alloy backing and Silastic insert) in an unbounded water phantom were performed using MCNP5 and BrachyDose with the level of detail described in Refs. 19 and 20.

II.A. TG-43-based brachytherapy treatment planning

In calculation method (1a) above, the 1D formalism utilized a 1D anisotropy function of unity at all radii r as in $\phi_{an}(r)=1$ [Eq. (1)], while calculation method (2a) above used the 2D formalism [Eq. (2)], where all symbols for dosimetry parameters have the standard meanings from the 2004 AAPM TG-43U1 report,[1]

$$\dot{D}(r) = S_K \cdot \Lambda \cdot \left(\frac{r}{r_0}\right)^2 \cdot g_P(r) \cdot \phi_{an}(r), \tag{1}$$

$$\dot{D}(r,\theta) = S_K \cdot \Lambda \cdot \frac{G_L(r,\theta)}{G_L(r_0,\theta_0)} \cdot g_L(r) \cdot F(r,\theta). \tag{2}$$

Log-linear interpolation was used to obtain radial dose function $g_P(r)$ and $g_L(r)$ data for TPS input data with the 1D and 2D formalisms, respectively, for 59 data points between 1.0 mm $\leq r \leq$ 30.0 mm in 0.5 mm steps. The same r range with θ resolution of 10° was generally used for the 2D anisotropy function $F(r,\theta)$ with bilinear-linear interpolation over r and θ. The $g_L(r)$ and $F(r,\theta)$ data were based on the study of Dolan *et al.* (2006) and Monroe and Williamson (2002) for the model 6711 ^{125}I and model 200 ^{103}Pd sources, respectively.[26,27] These data are similar to those recommended in the 2004 AAPM TG-43U1 report; the Dolan *et al.* data were not yet available in 2004 and are considered more accurate than the data recommended for the model 6711 in the 2004 TG-43U1 report. Both datasets used in the present

study are in good agreement with the data of Taylor *et al.*[28,29]

Due to limited precision of data entry by some TPS, especially for the dose-rate constant Λ, the model 6711 ^{125}I source was described with an active length L of 2.8 mm, half-life of 59.4 days, $\Lambda=0.96$ cGy h^{-1} U^{-1}, and air-kerma strength $S_K=4.572$ U. These parameters were chosen to obtain a dose of approximately 85 Gy for an irradiation time of 100 h to a central-axis depth d of 5 mm where the distance d is the distance along the plaque central-axis from the inner sclera (in contrast with r which is the distance from the coordinate system origin of each source). Similarly, the model 200 ^{103}Pd source was described with $L=4.23$ mm, half-life of 16.99 days, $\Lambda=0.69$ cGy h^{-1} U^{-1}, and $S_K=3.879$ U to obtain approximately 85 Gy to $d=5$ mm for an irradiation time of 168 h. These irradiation times were taken as representative for readily available source strengths of ^{125}I and ^{103}Pd. Source strengths up to 6.8 U for ^{103}Pd are available with short lead-times, resulting in irradiation times closer to the 100 hours used for ^{125}I in this study. Details concerning the three TG-43 based TPS (i.e., Pinnacle, BrachyVision, and PS) are outlined below. The degree of agreement among TPS depends partially on the fact that all systems used the same input data which in turn were consistent with the MC calculations performed in water. If different data were input, the results (given below) may not be in such good agreement.

II.A.1. Pinnacle

Brachytherapy dose calculations using Pinnacle (Philips Medical Systems, Cleveland, OH) were performed with version 8.0dp1; although, the brachytherapy dose calculation module has not changed between version 6.0g (2001) and version 9 (2009). The $g_P(r)$, $g_L(r)$, and $F(r,\theta)$ values were tabulated for 0.5 mm$\leq r\leq$30.0 mm in 0.5 mm steps (60 entries), and 5° angular sampling was used for $F(r,\theta)$ (1140 total entries). When using a dose grid of 0.5 mm or 1.5 mm, or with $F(r,\theta)$ having 5° or 10° sampling, dose values at all positions remained constant within 0.5%. Along-and-away lookup tables for all source models were calculated using 0.1 mm steps between 0.0 mm and 30.0 mm, utilizing 90,601 data points per source model. While the TG-43 calculation methodology was utilized to generate the lookup table, the table was subsequently employed in treatment planning calculations using the superposition principle. A dose calculation grid of 0.5 mm was set within the application for the display of isodose lines.

II.A.2. BrachyVision

Brachytherapy dose calculations for both ^{103}Pd and ^{125}I sources were performed using two different versions (6.1 and 8.1) of BrachyVision (Varian Medical Systems, Palo Alto, CA). In comparison to version 6.1, version 8.1 has higher precision in dosimetry parameter data entry. Further, the newer version corrected truncation errors of source coordinates and point-dose calculations. Consequently, only v.8.1 results are included herein. A 1.0 mm dose grid was specified. Values of $g_P(r)$ and $g_L(r)$ were entered with spatial resolutions of 0.5 mm for 0.5 mm$\leq r\leq$10 mm and at 5 mm for 15 mm$\leq r\leq$50 mm, totaling 28 entries. Values of $F(r,\theta)$ had 5° resolution for $0°\leq\theta\leq 90°$, and 1.0 mm radial resolution for 1 mm$\leq r\leq$50 mm, utilizing 950 entries. It was found that using smaller radial and angular increments altered results by $<0.2\%$.

II.A.3. Plaque Simulator

Brachytherapy dose calculations were performed using version 5.3.9 of PS. For the model 6711 ^{125}I seed, $g_P(r)$ and $g_L(r)$ values were entered at 0.5 mm intervals for 0.5 mm $\leq r\leq 3$ mm, at 1 mm intervals for 4 mm$\leq r\leq$10 mm, and at 5 mm intervals for 15 mm$\leq r\leq$40 mm. Values of $F(r,\theta)$ values were entered at 5° intervals and at seven radial distances, r=2.5, 5, 10, 20, 30, 40, and 50 mm. For the model 200 ^{103}Pd seed, $g_P(r)$ and $g_L(r)$ values were entered using the following radial spacing: r=1, 1.5, 2, 2.5, 3, 4, 5, 7.5, and 10 mm, and 5 mm intervals for 15 mm$\leq r\leq$40 mm. The values of $F(r,\theta)$ were entered at nonuniform intervals in order to provide more angular detail near the source long-axis at θ=0°, 1°, 2°, 3°, 5°, 7°, 10°, 12°, 15°, 20°, 25°, 30°, 40°, 50°, 60°, 70°, 75°, 80°, 85°, and 90° and r=2.5, 5, 10, 20, 30, 40, and 50 mm. The dose grid was 0.25 mm.

Besides the TG-43-based dose calculation, plaque heterogeneity correction functions were incorporated in the PS dose calculation using optional modules. Dose collimation by the lip on the gold-alloy backing was enabled. The analytical dose correction function $T(r)$ was used in dose calculations for individual seeds to account for combined effects of the gold-alloy backing and Silastic carrier insert. Values of $T(r)$ were obtained from a fit to the dose ratio with and without the gold-alloy backing and Silastic insert for a single seed in the center slot of a 20 mm COMS plaque as obtained from MC calculations by Thomson and Rogers using the BrachyDose code.[30] Based on the results obtained by Thomson *et al.*,[20] these dose ratios vary by less than 1% for 12 mm and 20 mm plaques over the range of interest, thus allowing a single table for each seed model appropriate for use with all plaque sizes. In combination with $T(r)$, an additional path length correction was used to account for oblique Silastic thicknesses greater than 1 mm.

II.B. Monte Carlo eye plaque simulations

For the MC simulations, absorbed dose was approximated as collision kerma due to the low photon energies and short secondary charged particle (electron) ranges. Section II A lists the radionuclide half-lives, seed S_K values, and irradiation times used subsequent to MC simulations of the dose per history to determine the dose for the specified treatment times. To ensure consistent normalization with TPS dose calculations, MC-derived doses were scaled by the ratio Λ/Λ_{MC}, where Λ was the value of the dose-rate constant used for TPS dose calculations and Λ_{MC} was the value of the dose-rate constant derived with the appropriate MC code[19,20] which differed slightly (e.g., by -3.8% and $+0.6\%$ for ^{125}I and ^{103}Pd, respectively, for the BrachyDose calculations) from those selected for the current study.

II.B.1. MCNP5

The MCNP5 (v1.40) simulations were performed according to the methods of Melhus and Rivard for a fully loaded 16 mm COMS eye plaque containing either ^{125}I model 6711 or ^{103}Pd model 200 brachytherapy sources.[19] The simulations employed the same plaque and seed geometry, but varied the tally mesh (a track-length estimate of the particle flux averaged over a mesh cell) to include a lateral extent of ± 12.4 mm and longitudinal extent (parallel to the central-axis) from -5 mm to 24.2 mm with $(0.2\ \text{mm})^3$ cubic voxels. A total of 10^9 particles were simulated to achieve central-axis statistical uncertainties ($k=1$) of $<0.5\%$ at the inner sclera, 0.9% at $d=5$ mm on the central-axis, and 2% at the opposite retina.

II.B.2. BrachyDose

The EGSnrc user-code BrachyDose (BD) was used to perform MC simulations which fully modeled brachytherapy seeds and COMS-plaques.[20] Seed models in homogeneous water medium were previously benchmarked.[28,29] Plaques were simulated at the center of a cubic water phantom of edge length 300 mm. Dose was scored in $(0.5\ \text{mm})^3$ cubic voxels using a track-length estimator. Simulations with 10^{10} histories were performed, resulting in statistical uncertainties ($k=1$) of $<0.05\%$ at the inner sclera, $<0.1\%$ at $d=5$ mm on the central-axis (tumor apex), and 0.5% at the opposite retina and other points of interest.

II.C. Plaque and eye models

The dose-distribution calculations were limited to a 16 mm COMS-plaque at different positions on the eye. Based on clinical experience, the 16 mm COMS plaque is one of the most frequently used plaque sizes among the various COMS sizes currently available from 10 mm to 22 mm diameters, in 2 mm increments.[12] With the assumptions used in the COMS, the right eye was modeled as a 24.6 mm diameter water sphere. The inner sclera and outer sclera were set to $d=0$ mm and $d=-1$ mm, respectively, along the central-axis. The plaque and eye schematic shown in Fig. 1 depict positions where doses were calculated. The plaque was loaded with 13 radioactive seeds as shown in Fig. 2. Centers of the sources were placed at a radius of 13.7 mm in a Silastic insert with a total thickness of 2.2 mm and an approximate 1 mm cover for each seed. The Silastic density was taken as $1.12\ \text{g/cm}^3$ and its composition was taken as 6.3% H, 24.9% C, 28.9% O, 39.9% Si, and 0.005% Pt by weight.[13] The coordinates of 13 seeds, including seed centers and end points, are listed in Table I for the 16 mm COMS plaque. The plaque's central-axis passed through the tumor apex taken to be at $d=5$ mm. Dose values along the central-axis are reported at $d=-1$, 0, 1, 2, 3, 4, 5, 6, 7, 8, 9, 10, 11.3, 15, 20, and 22.6 mm. The eight following plaque positions on the standardized right eye were simulated for dose comparisons:

(1) centered on equator on temporal side (9 o'clock);
(2) centered on equator on nasal side (3 o'clock);

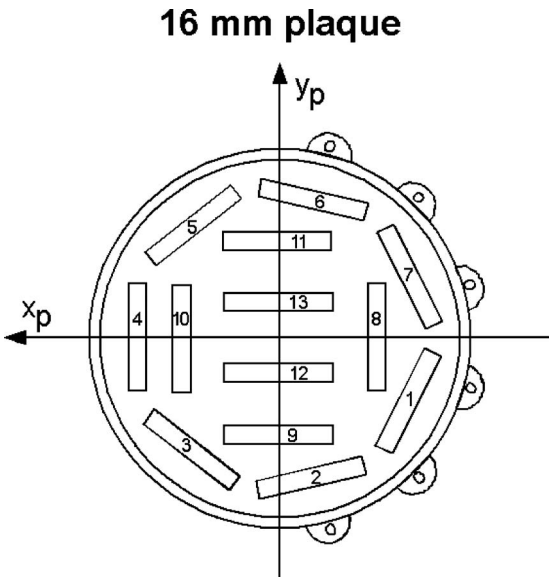

FIG. 2. Seed diagram (in x_p, y_p plane) viewed from the convex side of the Silastic insert of the 16 mm COMS standard eye plaque. The plaque's central-axis z_p is pointing into the page/screen (i.e., into the eye). The open rectangles labeled by numbers designate the seeds, whose coordinates are listed in Table I. For each plaque, there are six suture lugs shown on the right side of the plaque.

(3) centered on equator on superior side (12 o'clock);
(4) centered on equator on inferior side (6 o'clock);
(5) posterior to equator on temporal side (9 o'clock);
(6) posterior to equator on nasal side (3 o'clock, Fig. 1);
(7) posterior to equator on superior side (12 o'clock);
(8) posterior to equator on inferior side (6 o'clock).

For the first four positions [(1)–(4)], "centered on equator" means the plaque's central-axis is on the equatorial plane of a standardized right eye. For the second four positions [(5)–(8)], "posterior to equator" means that the plaque's center is between the equatorial plane and the posterior pole where the macula and fovea are located. The corresponding retinal diagrams, also called fundus diagrams,[31] for these eight tumor and plaque positions are shown in Fig. 3. The 2D cross-sectional diagram and 3D rendering of a 16 mm COMS-plaque at position #6 are shown in Figs. 1(a) and 1(b), respectively.

For each plaque position, points-of-interest doses for organs at risk are reported for the fovea, optic disk center, lens center, and lacrimal gland center with coordinates (in millimeters) in the eye coordinate system (X, Y, Z) of $(-11.3, 0, 0)$, $(-10.6, 4, 0)$, $(7.7, 0, 0)$, and $(7.7, -8.2, 8.2)$, respectively. The eye center and opposite retina are on the plaque's central-axis at $d=11.3$ mm and $d=22.6$ mm, respectively. Isodose contours in the horizontal plane intersecting the eye center for a plaque in position #1 are presented based on data produced with BrachyDose (BD) simulations. Contours for the dose in Gy for BD-Homo and BD-Hetero are presented (with dose normalized to 85 Gy at the tumor apex for BD-Homo), as well as the percentage difference between BD-Homo and BD-Hetero dose distributions: 100% x [BD-Homo–BD-Hetero]/BD-Homo.

TABLE I. Coordinates (millimeters) of seeds in the 16 mm COMS standard eye plaque. The seed physical length was set to 4.5 mm. Physical positioning of the seed # assignment is shown in Fig. 2. The COMS reference coordinate system origin at ($x_p=0$, $y_p=0$, $z_p=0$) is defined at the inner sclera along the plaque's central-axis. For MC calculations, the slightly longer 6711 seeds were centered with the same orientation.

Seed	Seed center coordinates			Seed end coordinates					
	x_{pc}	y_{pc}	z_{pc}	x_{p1}	y_{p1}	z_{p1}	x_{p2}	y_{p2}	z_{p2}
1	−5.68	−2.73	−0.87	−6.65	−0.71	−0.87	−4.70	−4.76	−0.87
2	−1.40	−6.14	−0.87	−3.60	−5.64	−0.87	0.79	−6.64	−0.87
3	3.93	−4.93	−0.87	2.17	−6.33	−0.87	5.69	−3.52	−0.87
4	6.30	0.00	−0.87	6.30	−2.25	−0.87	6.30	2.25	−0.87
5	3.93	4.93	−0.87	5.69	3.52	−0.87	2.17	6.33	−0.87
6	−1.40	6.14	−0.87	0.79	6.64	−0.87	−3.60	5.64	−0.87
7	−5.68	2.73	−0.87	−4.70	4.76	−0.87	−6.65	0.71	−0.87
8	−4.50	0.00	−1.64	−4.50	2.25	−1.64	−4.50	−2.25	−1.64
9	0.00	−4.50	−1.64	−2.25	−4.50	−1.64	2.25	−4.50	−1.64
10	4.50	0.00	−1.64	4.50	−2.25	−1.64	4.50	−2.25	−1.64
11	0.00	4.50	−1.64	2.25	4.50	−1.64	−2.25	4.50	−1.64
12	0.00	−1.80	−2.28	−2.25	−1.80	−2.28	2.25	−1.80	−2.28
13	0.00	1.80	−2.28	2.25	1.80	−2.28	−2.25	1.80	−2.28

III. RESULTS

III.A. Central-axis

Table II presents absolute dose along the plaque's central-axis calculated by each method using the initial conditions described in Sec. II. Taken as the average of the standard deviation of doses from the mean at points along the central-axis, agreement among the Point-Homo methods for ^{125}I and ^{103}Pd is 0.1% and 0.5%, respectively, with 0.6% and 1.1% agreement among Line-Homo methods, respectively. At any point on the central-axis, the average of doses calculated with the three Point-Homo and five Line-Homo approaches differed negligibly (~0.1%) for ^{125}I and ~1% for ^{103}Pd. At each depth the average dose calculated by the three TPS was generally within 2% of that calculated by the MC codes for both seed-types examined, which is within the expected total dosimetric uncertainties for these techniques. The average dose ratio of PS-Hetero to MC-Hetero along the central-axis (-1 mm$<d<22.6$ mm) is 0.991 ± 0.010 for ^{125}I and 1.010 ± 0.019 for ^{103}Pd. The last column of Table II indicates dose reductions due to heterogeneities (calculated as the average dose in MC-Hetero) relative to the average doses for the Point-Homo calculations for the fixed source strengths. At the prescription point ($d=5$ mm), the plaque's presence reduces doses by 11% and 20% for ^{125}I and ^{103}Pd, respectively, compared with Point-Homo calculations of 85 Gy to the same location. This results in delivered doses at $d=5$ mm of 76 Gy and 67 Gy for ^{125}I and ^{103}Pd, respectively. Dose calculated along the central-axis for -1 mm$<d<22.6$ mm using MC simulations to account for the plaque's heterogeneity and interseed perturbations are lower than homogeneous plan values by about 11%–20% for ^{125}I and 20%-37% for ^{103}Pd. These dose reductions, due to the plaque's heterogeneity effects, are in agreement with those observed by Melhus and Rivard[19] and by Thomson *et al.*[20] The magnitudes of dose reductions on the central-axis, in particular, the dose reductions of 9 Gy and 18 Gy at the prescription point ($d=5$ mm) for ^{125}I and ^{103}Pd, respectively, are significant. However, these dose differences have been present all along and indicate the most accurate estimate of the current administered dose given a current written directive prescribing 85 Gy to $d=5$ mm using the AAPM TG-43 dose calculation formalism.

III.B. Off-axis

For off-axis locations and the different plaque positions investigated, Table III presents the average results from the different TPS and MC codes for each calculation type (i.e., Point-Homo, Line-Homo, and MC-Hetero). As expected, doses at off-axis points of interest in a homogeneous medium are lower for line-source approximations as compared to point-source approximations. The largest deviations are found at the lacrimal gland center, where the line-source approximation results in 10% and 20% less dose than the point-source approximation for ^{125}I and ^{103}Pd sources, respectively. The inclusion of plaque heterogeneities from the gold-alloy backing and Silastic insert (i.e., MC-Hetero) causes dose reductions of approximately 20%–30% for most points of interest, and up to 92% (a factor of 12) dose reductions at off-axis positions such as the lacrimal gland center (positions #1 and #3, Table III). Doses to the four points of interest for organs at risk are considerably lower for ^{103}Pd than for ^{125}I for all eight plaque configurations.

At positions #5–#8 (Table III), the maximum point of interest doses using the MC-Hetero technique are for the fovea and optic disk and are approximately 59 Gy and 48 Gy for ^{125}I and 45 Gy and 35 Gy for ^{103}Pd, respectively. When visual acuity is an important end point, dose to these structures should be minimized. In this case, the accuracy of dose calculation can have a major influence on the magnitude of corrections due to the limitations of TG-43 based methods

TABLE II. Central-axis dose values in Gy for a COMS 16 mm eye plaque loaded with (top) 13 ^{125}I sources (model 6711, 4.572 U each) and (bottom) 13 ^{103}Pd sources (model 200, 3.879 U each) for Pinnacle (P^3) version 8.0dp1, BrachyVision (BV) version 8.1, Plaque Simulator (PS) version 5.3.9, MCNP5 (MCNP) version 1.40, and BrachyDose (BD). Values are calculated using Point-Homo and Line-Homo for the 1D and 2D TG-43 dosimetry formalisms, respectively, using homogeneous water phantoms, and PS-Hetero and MC-Hetero using heterogeneous phantoms. The ratio of average MC-Hetero/Point-Homo (with MC-Hetero equal to the average MCNP and BD results) is given in the last column.

		Point-Homo			Line-Homo					PS-Hetero or MC-Hetero			
d (mm)	CAX points	P^3	BV	PS	P^3	BV	PS	MCNP	BD	PS	MCNP	BD	$\left(\frac{\text{MC-Hetero}}{\text{Point-Homo}}\right)$
^{125}I −1.0	Outer sclera	340	339	341	341	340	339	342	341	276	273		0.80
0.0	Inner sclera	261	261	261	261	261	260	261	262	225	224	222	0.86
1.0		203	203	203	203	203	202	206	204	178	181	177	0.88
2.0		161	161	161	161	161	160	162	161	141	143	141	0.88
3.0		129	129	129	129	129	128	129	129	113	114	114	0.89
4.0		104	104	104	104	104	103	104	104	91.3	92.0	91.5	0.89
5.0	Rx depth	84.4	84.5	84.5	84.4	84.5	83.9	85.6	84.7	74.0	75.8	74.3	0.89
6.0		69.2	69.2	69.3	69.2	69.2	68.8	69.5	69.5	60.4	61.4	60.8	0.88
7.0		57.2	57.2	57.3	57.2	57.2	56.9	57.9	57.4	49.7	51.0	50.1	0.88
8.0		47.7	47.7	47.7	47.7	47.7	47.4	47.3	47.9	41.2	41.3	41.5	0.87
9.0		40.0	40.0	40.1	40.0	40.0	39.8	40.2	40.3	34.5	34.8	34.8	0.87
10.0		33.9	33.9	33.9	33.9	33.9	33.7	34.2	34.2	29.0	29.6	29.3	0.87
11.3	Eye center	27.6	27.6	27.7	27.6	27.6	27.5	27.8	27.9	23.5	24.1	23.8	0.87
15.0		16.3	16.3	16.4	16.3	16.3	16.3	16.7	16.5	13.7	14.2	13.9	0.86
20.0		8.87	8.89	8.90	8.87	8.89	8.84	8.90	9.02	7.32	7.57	7.40	0.84
22.6	Opposite retina	6.70	6.71	6.71	6.70	6.70	6.67	6.68	6.81	5.49	5.45	5.57	0.82
^{103}Pd −1.0	Outer sclera	349	350	347	349	349	349	342	350	228	214		0.63
0.0	Inner sclera	278	279	278	278	279	274	270	275	207	200	201	0.73
1.0		217	218	216	217	218	214	210	214	168	164	165	0.76
2.0		169	170	169	169	170	167	165	167	134	131	131	0.78
3.0		132	133	132	132	133	131	129	131	106	105	104	0.79
4.0		104	105	104	104	105	103	102	103	83.6	82.8	82.6	0.79
5.0	Rx depth	82.5	83.0	82.6	82.5	83.0	81.5	80.9	81.1	66.3	65.8	65.5	0.80
6.0		65.6	66.0	65.7	65.6	66.0	64.8	65.0	64.6	52.7	53.6	52.2	0.80
7.0		52.5	52.8	52.6	52.6	52.8	51.9	52.4	51.8	42.2	43.1	41.8	0.80
8.0		42.4	42.8	42.6	42.4	42.6	42.0	42.0	41.8	34.1	34.5	33.7	0.80
9.0		34.5	34.9	34.7	34.5	34.6	34.3	34.7	33.9	27.8	28.1	27.4	0.80
10.0		28.2	28.6	28.5	28.2	28.4	28.1	28.0	27.9	22.7	22.7	22.3	0.80
11.3	Eye center	22.0	22.3	22.2	22.0	22.3	21.9	22.6	21.8	17.6	18.3	17.4	0.79
15.0		11.5	11.6	11.6	11.4	11.5	11.4	11.6	11.4	9.13	9.38	8.99	0.79
20.0		5.24	5.33	5.31	5.25	5.33	5.23	5.16	5.18	4.15	4.18	4.11	0.78
22.6	Opposite retina	3.62	3.65	3.64	3.62	3.65	3.59	3.62	3.55	2.84	2.88	2.80	0.78

without heterogeneity correction. For the aforementioned circumstances with ^{125}I and ^{103}Pd, these corrections are approximately 25% and 42%, respectively.

Figure 4 illustrates the calculated dose-discrepancies between homogenous and heterogeneous approaches with BD data for a 16 mm COMS plaque located at position #1. The isodose contours [Figs. 4(a) and 4(b)] are more conformal to the tumor volume for BD-Hetero than for BD-Homo calculations for both radionuclides. Figures 4(a) and 4(b) also illustrate the more rapid dose fall-off with distance from the plaque for ^{103}Pd than for ^{125}I, in accord with the results of Thomson *et al.*,[20] Thomson and Rogers,[30] and Melhus and Rivard.[19] Doses to critical points of interest and to regions surrounding the eye are lower with ^{103}Pd (model 200) than for ^{125}I (model 6711), with the exception of the inner sclera;[20] Thomson and Rogers reported lower doses to critical normal structures and surrounding tissues for all ^{103}Pd seed models than for ^{125}I seed models except at the sclera adjacent the plaque where doses vary with seed model and are not always higher for ^{103}Pd than for ^{125}I.[30] Figures 4(c) and 4(d) show the percentage difference for BD-Homo and BD-Hetero dose distributions; dose differences are significant in all regions of the eye and are particularly large in the plaque penumbral-region.

IV. DISCUSSION

Although only the 16 mm COMS plaque is examined in this study, others have reported on dose variations as a function of plaque diameter.[19,20] Central-axis MC heterogeneity corrections suggest that the ratio of heterogeneous to homogeneous dose calculations does not vary appreciably as a function of plaque diameter.[19,20] Melhus and Rivard[19] observed that the ratio of heterogeneous to homogeneous

TABLE III. Off-axis average dose values in Gy for a COMS 16 mm eye plaque for organs at risk (fovea, optic disk center, lens center, and lacrimal gland center) for eight different positions of the plaque (#1–#8, Fig. 3) loaded with 13 sources of ^{125}I (model 6711, LHS) and ^{103}Pd sources (model 200, RHS). Values were calculated using Point-Homo and Line-Homo for the 1D and 2D TG-43 dosimetry formalisms, respectively, in homogeneous water phantoms, and MC-Hetero for the MC simulations in a heterogeneous phantom.

		^{125}I					^{103}Pd				
Plaque position	Off-axis location	Point-Homo (Gy)	Line-Homo (Gy)	MC-Hetero (Gy)	$\left(\frac{\text{Line-Homo}}{\text{Point-Homo}}\right)$	$\left(\frac{\text{MC-Hetero}}{\text{Point-Homo}}\right)$	Point-Homo (Gy)	Line-Homo (Gy)	MC-Hetero (Gy)	$\left(\frac{\text{Line-Hetero}}{\text{Point-Homo}}\right)$	$\left(\frac{\text{MC-Hetero}}{\text{Point-Homo}}\right)$
#1	Fovea	16.7	16.3	12.8	0.98	0.77	12.0	11.0	7.8	0.92	0.65
	Optic disk	11.3	11.2	9.0	1.00	0.80	7.2	6.9	5.1	0.95	0.71
	Lens	21.6	21.5	18.0	0.99	0.83	16.5	15.7	11.9	0.95	0.72
	Lacrimal Gland	43.4	39.2	6.1	0.90	0.14	39.3	30.7	3.3	0.78	0.08
#2	Fovea	16.7	16.3	12.8	0.98	0.77	12.0	11.0	7.8	0.92	0.65
	Optic disk	28.8	27.6	21.0	0.96	0.73	23.8	20.9	13.8	0.88	0.58
	Lens	21.6	21.5	18.0	0.99	0.83	16.5	15.7	11.9	0.95	0.72
	Lacrimal Gland	7.1	7.1	5.7	1.00	0.80	4.0	3.9	2.9	0.98	0.73
#3	Fovea	16.7	16.3	12.8	0.98	0.77	12.0	11.0	7.8	0.92	0.65
	Optic disk	16.6	16.3	12.8	0.98	0.77	12.0	11.0	7.8	0.92	0.66
	Lens	21.6	21.5	18.0	0.99	0.83	16.5	15.7	11.9	0.95	0.72
	Lacrimal Gland	43.4	39.2	6.1	0.90	0.14	39.3	30.7	3.3	0.78	0.08
#4	Fovea	16.7	16.3	12.8	0.98	0.77	12.0	11.0	7.8	0.92	0.65
	Optic disk	16.6	16.3	12.8	0.98	0.77	12.0	11.0	7.8	0.92	0.66
	Lens	21.6	21.5	18.0	0.99	0.83	16.5	15.7	11.9	0.95	0.72
	Lacrimal Gland	7.1	7.1	5.7	1.00	0.80	4.0	3.9	2.9	0.98	0.73
#5	Fovea	77.7	73.8	58.7	0.95	0.76	76.8	66.5	44.9	0.87	0.58
	Optic disk	32.5	31.0	23.4	0.95	0.72	27.6	24.1	15.7	0.87	0.57
	Lens	12.0	12.2	10.3	1.01	0.85	7.8	7.7	6.0	0.99	0.77
	Lacrimal Gland	13.7	13.3	9.0	0.96	0.65	9.4	8.4	4.8	0.89	0.51
#6	Fovea	28.3	27.1	20.8	0.96	0.73	23.3	20.5	13.6	0.88	0.59
	Optic disk	62.5	59.3	45.9	0.95	0.73	60.0	51.7	34.1	0.86	0.57
	Lens	15.8	15.9	13.3	1.00	0.84	11.1	10.8	8.3	0.97	0.74
	Lacrimal Gland	6.3	6.3	5.1	1.01	0.82	3.3	3.3	2.5	0.98	0.74
#7	Fovea	77.7	73.8	58.7	0.95	0.76	76.8	66.5	44.9	0.87	0.58
	Optic disk	63.7	60.4	47.8	0.95	0.75	61.1	52.0	34.5	0.85	0.56
	Lens	12.0	12.2	10.3	1.01	0.85	7.8	7.7	6.0	0.99	0.77
	Lacrimal Gland	13.7	13.3	9.2	0.97	0.67	9.4	8.4	4.8	0.89	0.51
#8	Fovea	77.7	73.8	58.7	0.95	0.76	76.8	66.5	44.9	0.87	0.58
	Optic disk	63.4	60.5	47.5	0.95	0.75	60.8	51.9	34.3	0.85	0.56
	Lens	12.0	12.2	10.3	1.01	0.85	7.8	7.7	6.0	0.99	0.77
	Lacrimal Gland	5.9	6.0	4.9	1.01	0.82	3.1	3.1	2.3	0.99	0.75

313

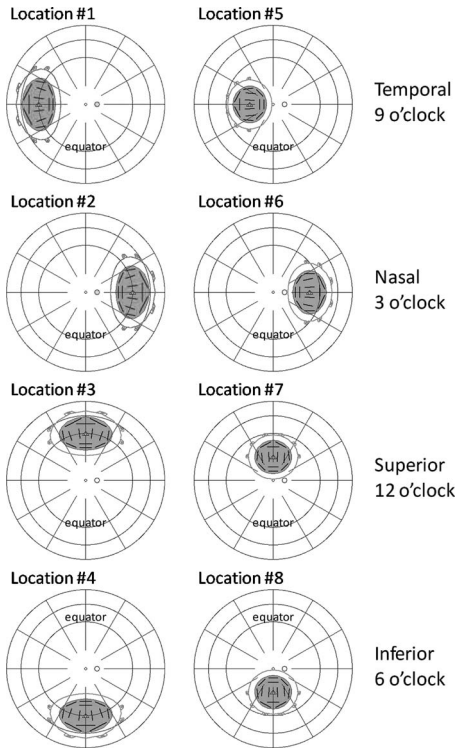

FIG. 3. Retinal diagrams (also called fundus diagrams) looking from the front into the eye showing the eight different positions (#1–#8) of plaques and suture points on the right eye. The center in each diagram indicates the fovea, which is the center of macula. The small circle on the nasal side of the fovea represents the optic disk. The innermost of the three circles indicates the equator of the eye. The labels on the right describe the position of the tumor/plaque on the right eye. For example, positions #1 and #5 (top graphs) are at the temporal side of the right eye at 9 o'clock.

central-axis dose across seven plaque sizes had a standard deviation ($k=1$) less than 2% for the model 6711 source and less than 3% for the model 200 source. The largest differences are at the outer sclera, and differences in these ratios are less than or equal to 1% for both sources at depths of 1–10 mm from the inner sclera. These results are supported by Thomson *et al.*[20] In contrast, MC heterogeneity corrections for off-axis locations are generally more sensitive to plaque size than on-axis corrections due to variations in penumbra with plaque diameter. While the dose to the outer sclera relative to the prescription dose is significantly higher for 10–14 mm plaques, dose to the outer sclera as reported in these 16 mm comparisons is typical of the 16 mm and larger plaques.[19] Therefore, the results for 16 mm plaque presented here will not be identical to those for other plaque diameters, especially at off-axis locations.

These findings suggest that the lens dose for plaque positions #1–#4 can be significantly different from those calculated using current widely used dosimetry methods. This will affect scientific evaluations such as dose response and radiation-induced retinopathy and cataract.[4,32] When comparisons of normal tissue toxicity and administered doses are made with other treatment modalities such as external-beam photon or proton radiotherapy, accuracy of dose calculations becomes even more crucial.

In this study, we focused on a particular, widely used seed model for each of the radionuclides. This was motivated by the results from a recent study by Thomson and Rogers who reported on the variation of dose distributions for eye plaque therapy as a function of seed model.[30] They identified six seed models to have sufficient air-kerma strength for eye plaque therapy.[30] In their study, dose decreases relative to homogeneous TG-43 assumptions varied only slightly with seed model, demonstrating variations up to 2%. Points of interest doses are lower for ^{103}Pd seed models than with ^{125}I with the possible exception of the sclera. Based on the results of the study by Thomson and Rogers, results presented herein for the specific models of ^{125}I and ^{103}Pd sources are typical of other similar source models. Regardless, the decrease in dose to the four points of interest for organs at risk from ^{103}Pd in comparison to ^{125}I was expected due to the lower penetration of ^{103}Pd photons with lower average photon energy than ^{125}I.

This study focused on the dosimetry of a COMS plaque for which extensive high quality clinical outcome data are available in the literature.[4,9,16,32] Following the COMS trials, many clinical studies using variations of eye plaques have reported equivalent or better clinical outcomes. It may be useful to reanalyze their dosimetry using modern MC methods. Dosimetry for plaques of other models will generally differ considerably from dosimetry for COMS-style plaques.[33] Heterogeneity corrections depend critically on plaque design and can be significant in magnitude. For example, Thomson *et al.*[33] recently reported calculated dose distributions for treating iris melanoma using several plaque designs which are drastically different from those for COMS; they found that although dose distributions computed under the TG-43 approach are identical, doses computed with MC methods (with plaques fully modeled) differ substantially.

It should be noted that the issues regarding the impact on the prescription dose following the adoption of MC-based calculations also apply to the adoption of PS with the heterogeneity corrections turned on. PS users are perhaps at risk of overdosing patients up to 20% if heterogeneity corrections are used and the prescribed dose is not modified appropriately. This issue is a major topic of interest for the upcoming report of an AAPM Task Group (TG-129).

Many clinics currently prefer to use plaques that are thinner than the original COMS design and other models are manufactured without lipped edges. Also, many users no longer use a Silastic insert. Therefore, since the quantitative dosimetry conclusions reported in this work are specific to the standard COMS plaque design, they may not apply to different designs—particularly if used in a non-COMS fashion. Regardless of plaque design, we expect that the lower energy ^{103}Pd-derived photons are less likely to reach most normal ocular structures compared to ^{125}I. The approximate 10% and 20% dose reductions at the prescription point for ^{125}I and ^{103}Pd, respectively, warrant attention by the medical community using eye plaque brachytherapy and should be considered in the context of clinical standards and local control rates at each institution when the clinics adopt MC dose calculation methods for clinical dosimetry.

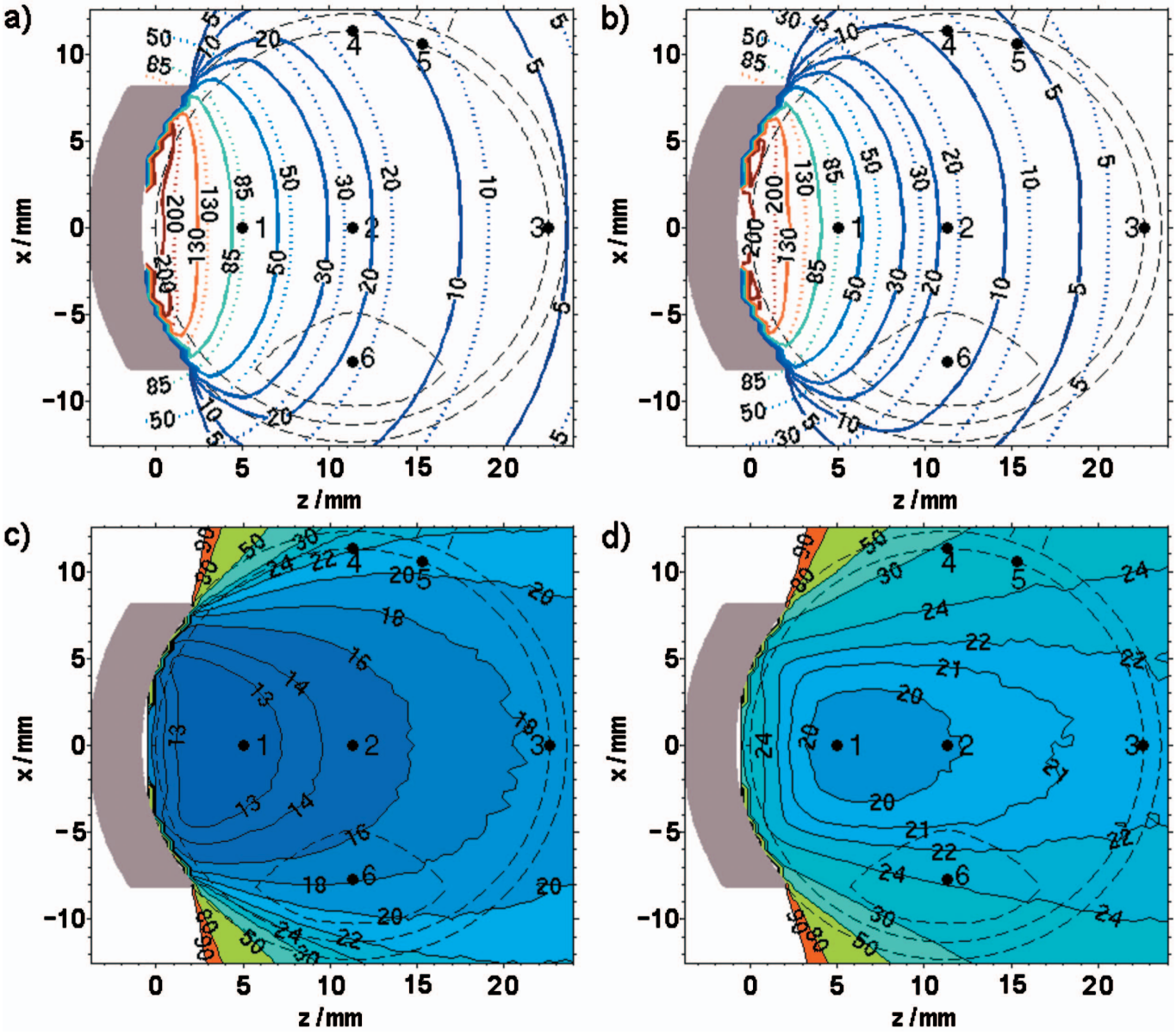

FIG. 4. Isodose contours in the horizontal plane intersecting the eye center for a 16 mm COMS plaque on the equator temporal of the right eye (position #1) fully loaded with ^{125}I model 6711 [(a) upper left] or model 200 ^{103}Pd [(b) upper right] seeds. These absorbed dose data were produced with BrachyDose (BD) simulations of BD Line-Homo (seeds fully modeled in water; no interseed effects) and BD MC-Hetero (plaque and seeds fully modeled, includes interseed effects); dose was scored in (0.5 mm)^3 voxels in the eye region and was set to zero in voxels intersecting the plaque for BD-Hetero. Plots (a) and (b) provide isodose contours in Gy for BD Line-Homo (dotted lines) and BD MC-Hetero (solid lines) with the dose normalized to deliver 85 Gy at the tumor apex (i.e., 5 mm) for BD Line-Homo calculations. Plots (c) (lower left) and (d) (lower right) provide the percentage difference between BD Line-Homo and BD MC-Hetero dose distributions: 100% x [Line-Homo – MC-Hetero]/Line-Homo. Points of interest in the eye are numbered as (1) tumor apex, (2) eye center, (3) opposite retina, (4) fovea, (5) optic disk, and (6) lens.

V. CONCLUSIONS

Five different dose calculation systems were compared for ophthalmic plaque brachytherapy dose calculations, and included Pinnacle v8.0dp1, BrachyVision v8.1 PS v5.3.9, and two MC codes (MCNP5 v1.40 and BrachyDose/EGSnrc). Comparisons of dose values at various points along the plaque's central-axis and at off-axis points of interest (optic disk center, lacrimal gland center, fovea, and lens center) were made for a COMS 16 mm eye plaque loaded with 13 ^{125}I (model 6711) or ^{103}Pd (model 200) seeds. The plaque was placed at eight different positions on a model eye. Dose differences between TG-43 based conventional TPS and MC codes exceeding 10% are observed and increased up to 92% for dose points located further away at off-axis locations where shielding is not accounted for. These results help justify consideration of TPS using advanced dose calculation algorithms based on MC methods to more accurately predict dose delivered to patients with intraocular melanoma undergoing plaque brachytherapy.

ACKNOWLEDGMENTS

We extend our appreciation to Melvin Astrahan for assistance with source coordinate transformation and the avail-

ability of a trial license for the new version of PS prior to release, David Followill for insight on the COMS dosimetry standards, and to Laura Doyle, James Eddy, and Michael Parish for assistance with some of the BrachyVision calculations. This study was supported in part by The Eye Cancer Foundation, Inc. (http://eyecancerfoundation.net).

[a]Electronic mail: mrivard@tuftsmedicalcenter.org

[1]M. J. Rivard, B. M. Coursey, L. A. DeWerd, W. F. Hanson, M. S. Huq, G. S. Ibbott, M. G. Mitch, R. Nath, and J. F. Williamson, "Update of AAPM Task Group No. 43 Report: A revised AAPM protocol for brachytherapy dose calculations," Med. Phys. **31**, 633–674 (2004).

[2]M. J. Rivard, J. L. M. Venselaar, and L. Beaulieu, "The evolution of brachytherapy treatment planning," Med. Phys. **36**, 2136–2153 (2009).

[3]M. J. Rivard, L. Beaulieu, and F. Mourtada, "Necessary enhancements to commissioning techniques of brachytherapy treatment planning systems that use model-based dose calculation algorithms," Med. Phys. **37**, 2645–2658 (2010).

[4]P. T. Finger, K. J. Chin, and G.-P. Yu, "Risk factors for radiation maculopathy after plaque radiation for choroidal melanoma," Am. J. Ophthalmol. **149**, 608–615 (2010).

[5]P. T. Finger, "Tumour location affects the incidence of cataract and retinopathy after ophthalmic plaque radiation therapy," Br. J. Ophthamol. **84**, 1068–1070 (2000).

[6]J. Earle, R. W. Kline, and D. M. Robertson, "Selection of iodine 125 for the Collaborative Ocular Melanoma Study," Arch. Ophthalmol. (Chicago) **105**, 763–764 (1987).

[7]Collaborative Ocular Melanoma Study Group, COMS Manual of Procedures, Ch. 12: Radiation therapy, COMS manual of procedures PB95-179693 (National Technical Information Service, Springfield, VA, 1995).

[8]B. S. Hawkins, "The Collaborative Ocular Melanoma Study (COMS) randomized trial of pre-enucleation radiation of large choroidal melanoma: IV. Ten-year mortality findings and prognostic factors. COMS report number 24," Am. J. Ophthalmol. **138**, 936–951 (2004).

[9]COMS, "The COMS randomized trial of iodine 125 brachytherapy for choroidal melanoma: V. Twelve-year mortality rates and prognostic factors: COMS report No. 28," Arch. Ophthalmol. (Chicago) **124**, 1684–1693 (2006).

[10]R. Kline and J. Earle, "Implications of TG-43 for dose prescription and calculation for I-125 eye plaques," Med. Phys. **23**, 1054 (1996) (abstract).

[11]W. Hanson, "Implementation of the new I-125 standard and TG-43 recommendations in a cooperative clinical trial," Med. Phys. **23**, 1054 (1996) (abstract).

[12]S. Nag, J. M. Quivey, J. D. Earle, D. Followill, J. Fontanesi, and P. T. Finger, "The American Brachytherapy Society recommendations for brachytherapy of uveal melanomas," Int. J. Radiat. Oncol., Biol., Phys. **56**, 544–555 (2003).

[13]S.-T. Chiu-Tsao, L. L. Anderson, K. O'Brien, L. Stabile, and J. C. Liu, "Dosimetry for ^{125}I seed (model 6711) in eye plaques," Med. Phys. **20**, 383–389 (1993).

[14]S-T. Chiu-Tsao, L. L. Boulay, I. H. Kanna, A. de la Zerda, and J. H. Kim, "Dose distribution in the eye for ^{103}Pd COMS eye plaque," Med. Phys. **22**, 923 (1995) (abstract).

[15]A. de la Zerda, S. T. Chiu-Tsao, J. Lin, L. L. Boulay, I. Kanna, J. H. Kim, and H. S. Tsao, "^{125}I eye plaque dose distribution including penumbra characteristics," Med. Phys. **23**, 407–418 (1996).

[16]A. L. Krintz, W. F. Hanson, G. S. Ibbott, and D. S. Followill, "A reanalysis of the Collaborative Ocular Melanoma Study Medium Tumor Trial eye plaque dosimetry," Int. J. Radiat. Oncol., Biol., Phys. **56**, 889–898 (2003).

[17]M. A. Astrahan, G. Luxton, G. Jozsef, T. D. Kampp, P. E. Liggett, M. D. Sapozink, and Z. Petrovich, "An interactive treatment planning system for ophthalmic plaque radiotherapy," Int. J. Radiat. Oncol., Biol., Phys. **18**, 679–687 (1990).

[18]M. A. Astrahan, "Improved treatment planning for COMS eye plaques," Int. J. Radiat. Oncol., Biol., Phys. **61**, 1227–1242 (2005).

[19]C. S. Melhus and M. J. Rivard, "COMS eye plaque brachytherapy dosimetry simulations for ^{103}Pd, ^{125}I, and ^{131}Cs ," Med. Phys. **35**, 3364–3371 (2008).

[20]R. M. Thomson, R. E. Taylor, and D. W. O. Rogers, "Monte Carlo dosimetry for ^{125}I and ^{103}Pd eye plaque brachytherapy," Med. Phys. **35**, 5530–5543 (2008).

[21]M. J. Rivard, C. S. Melhus, S. Sioshansi, and J. Morr, "The impact of prescription depth, dose rate, plaque size, and source loading on the central-axis using ^{103}Pd, ^{125}I, and ^{131}Cs ," Brachytherapy **7**, 327–335 (2008).

[22]H. Zhang, D. Martin, S.-T. Chiu-Tsao, A. Meigooni, and B. R. Thomadsen, "A comprehensive dosimetric comparison between ^{131}Cs and ^{125}I brachytherapy sources for COMS eye plaque implant," Brachytherapy **9**, 362–372 (2010).

[23]X-5 Monte Carlo Team, *MCNP-A General Monte Carlo N-Particle Transport Code, Version 5* (Los Alamos National Laboratory, Los Alamos, NM, 2003).

[24]G. Yegin, R. E. P. Taylor, and D. W. O. Rogers, "BrachyDose: A new fast Monte Carlo code for brachytherapy calculations," Med. Phys. **33**, 2075 (2006) (abstract).

[25]I. Kawrakow and D. W. O. Rogers, "The EGSnrc code system: Monte Carlo simulation of electro and photon transport," NRC Report No. PIRS-701, Ottawa K1A 0R6, 2007, http://www.irs.inms.nrc.ca/inms/irs/EGSnrc/EGSnrc.html last accessed 5 December 2010.

[26]J. Dolan, Z. Li, and J. F. Williamson, "Monte Carlo and experimental dosimetry of an ^{125}I brachytherapy seed," Med. Phys. **33**, 4675–4684 (2006).

[27]J. I. Monroe and J. F. Williamson, "Monte Carlo-aided dosimetry of the Theragenics TheraSeed model 200 ^{103}Pd interstitial brachytherapy seed," Med. Phys. **29**, 609–621 (2002).

[28]R. E. P. Taylor, G. Yegin, and D. W. O. Rogers, "Benchmarking BrachyDose: Voxel based EGSnrc Monte Carlo calculations of TG-43 dosimetry parameters," Med. Phys. **34**, 445–457 (2007).

[29]R. E. P. Taylor and D. W. O. Rogers, "An EGSnrc Monte Carlo-calculated database of TG-43 parameters," Med. Phys. **35**, 4228–4241 (2008).

[30]R. M. Thomson and D. W. O. Rogers, "Monte Carlo dosimetry for ^{125}I and ^{103}Pd eye plaque brachytherapy with various seed models," Med. Phys. **37**, 368–376 (2010).

[31]S.-T. Chiu-Tsao, in *Brachytherapy Physics*, edited by B. R. Thomadsen, M. J. Rivard, and W. M. Butler (Medical Physics, Madison, Wisconsin, 2005), pp. 673–705.

[32]P. T. Finger, K. J. Chin, G.-P. Yu, and N. S. Patel, "Risk factors for cataract after palladium-103 ophthalmic plaque radiation therapy," Int. J. Radiat. Oncol., Biol., Phys. (in press).

[33]R. M. Thomson, K. M. Furutani, J. S. Pulido, S. L. Stafford, and D. W. O. Rogers, "Modified COMS plaques for ^{125}I and ^{103}Pd iris melanoma brachytherapy," Int. J. Radiat. Oncol., Biol., Phys. **78**, 1261–1269 (2010).